END
DATE
FILMED
6 80
DTIC

MICROCOPY RESOLUTION TEST CHART

NATIONAL BUREAU OF STANDARDS 1963 A

AFOSR-TR. 80-0334 **LEVEL** ③

Catoptrical X-Ray Optical System (For Use in Laser-Fusion Diagnostics)

ADA084688

ANNUAL TECHNICAL REPORT

1 October 1978 to 31 September 1979

Grant AFOSR 78-3480

Professor James F. McGee

X-Ray Optics Laboratory — *New*

Saint Louis University

St. Louis, Missouri 63103

DTIC

ELECTE

MAY 16 1980

D

411703

DC FILE COPY

80 5 14 009

REPORT DOCUMENTATION PAGE

READ INSTRUCTIONS
BEFORE COMPLETING FORM

1. REPORT NUMBER AFOSR-TR-80-0334	2. GOVT ACCESSION NO. AD-A084688	3. RECIPIENT'S CATALOG NUMBER

4. TITLE (and Subtitle)	5. TYPE OF REPORT & PERIOD COVERED
CATOPTRICAL X-RAY OPTICAL SYSTEM (For Use in Laser-Fusion Diagnostics)	Annual Technical Report Oct. 1, 1978 - Sept. 31,'79
	6. PERFORMING ORG. REPORT NUMBER

7. AUTHOR(s)	8. CONTRACT OR GRANT NUMBER(s)
Professor James F. McGee	AFOSR-78-3480

9. PERFORMING ORGANIZATION NAME AND ADDRESS	10. PROGRAM ELEMENT, PROJECT, TASK AREA & WORK UNIT NUMBERS
Department of Physics Saint Louis University 221 N. Grand Boulevard, St. Louis, Mo. 63103	61102F 2301-A7

11. CONTROLLING OFFICE NAME AND ADDRESS	12. REPORT DATE
Air Force Office of Scientific Research /NP Building 410 Bolling AFB, D.C. 20332	Dec 79
	13. NUMBER OF PAGES 28

14. MONITORING AGENCY NAME & ADDRESS(If different from Controlling Office)	15. SECURITY CLASS. (of this report)
	unclassified
	15a. DECLASSIFICATION/DOWNGRADING SCHEDULE

16. DISTRIBUTION STATEMENT (of this Report)

Approved for public release; distribution unlimited.

17. DISTRIBUTION STATEMENT (of the abstract entered in Block 20, if different from Report)

18. SUPPLEMENTARY NOTES

19. KEY WORDS (Continue on reverse side if necessary and identify by block number)

X-RAY OPTICS

LASER DIAGNOSTICS

20. ABSTRACT (Continue on reverse side if necessary and identify by block number)

A compound x-ray imaging device is being developed as an aid in the diagnostics of the laser fusion implosion process which involves a pellet of the order of 100 microns in diameter. Ideally, both temporal and spacial information is being sought. This report deals mainly with the removal of spherical aberration from a single x-ray optical element by means of a surface figure which is described by a polynomial of third order and higher. Such an x-ray focusing element would be useful in an X-Ray Streak camera for obtaining

DD FORM 1473
1 JAN 73

411763

20. Abstract (continued)

temporal information. Combinations of other higher-order surfaces and aperture stops will be used in a compound imaging-device in the attainment of spacial information with sub-micron resolution. Attention is given to the generation and testing of such high-order surfaces. A specially designed surface generator and lapping machine is described.

Accession For		
NTIS GRA&I		☒
DDC TAB		☐
Unannounced		☐
Justification		
By		
Distribution/		
Availability Codes		
Dist.	Avail and/or special	
A		

DTIC
SELECTED
MAY 16 1980
D

TABLE OF CONTENTS

I. Introduction:

A. Significance and Principal Aim of the Research

For some time now the need for a good scheme to image the x-rays associated with the laser-fusion implosion process of a thin spherical pellet in the 50 to 100 micron diameter range has been evident. Several laboratories have resorted to the age old pin-hole camera (literally a pin-hole in a sheet of lead which is positioned between the source and the recording film). Its quoted resolution of 15 microns by one source leaves much to be desired. A resolution at least two orders of magnitude lower would be desirable and attainable by x-ray focusing methods.

The principal investigator built the first successful long-wavelength x-ray microscope at Stanford while working under Professor Kirkpatrick. The microscope was capable of making x-ray micrographs of biological tissue-sections only seven microns thick with adequate contrast. In those days a detailed knowledge of the geometrical and physical optics connected with the formation of images by the total-external reflection of x-rays was only in its infancy, this particular phase of optics never having attracted the attention of the great optical scientists of bygone days.

Crossed-mirror x-ray microscopes as used by the author and others have been of the simple magnifier type. They lacked an ocular or eyepiece lens found in the ordinary compound light-microscope so common to biological laboratories. A compound microscope either for light or x-rays would be distinguished from a simple magnifier by the formation of an intermediate image.

Crossed-mirror x-ray microscopes have been used as simple magnifiers with one important difference. The object was placed just outside the first focal point so as to form a real magnified image which could be recorded on film.

We propose then the study and construction of a compound reflection x-ray system which will have sufficient resolution and magnification for laser fusion diagnostic purposes in the wavelength region of approximately 5 to 50 Å.

The compound x-ray microscope would be operated so that the real image formed by the objective lens would fall just outside of the focal point of the ocular or second lens so that the latter would produce a real image which could be recorded on film or by a vidicon or CCD.

Ordinarily we think of a telescope as an instrument which is used to examine large objects (moon) at large distances (moon to earth). A microscope on the other hand is used to examine small objects (a bacterium) at small distances (oil-immersion lens). The pellet used in laser fusion is indeed small (50 to 100 microns). However it is not feasible to examine it at very small distances, as it implodes, because of possible damage to the observing system from target debris and heat. With the latter realization the goal is modified to that of examining a small object at a large distance.

Occasionally biologists are faced with a similar need and will exchange their objective lens having a focal length of a fraction of a mm for one which has a focal length of 5 cm. The latter type of objective lens is referred to as a "large working distance" objective since now the specimen must be placed slightly greater than 5 cm from the objective lens.

A suitable x-ray imaging system for laser fusion diagnostics does indeed need an objective lens with a "large working distance". For instance in the Rochester tank no diagnostic apparatus can be closer than 22 cm to the target. Even more serious than this mechanical limitation is the fact that at calculated power output aluminum filter-foils would be vaporized and optical components otherwise damaged by target debris.

Due to the heating and debris constraints we are currently designing our apparatus so that no parts project within the tank. Our design working-distance will be 90 to 100 cm subject to change of course upon receipt of further information. The Rochester tank is 90 cm in radius with many ports about 5.08 cm in diameter.

II. Recent Work by the Principal Investigator and Students:

To date, all aberrations determinations for the focusing of x-rays by a concave spherical reflector or by concave cylindrical mirror of circular cross section have revealed serious spherical and obliquity aberration. The latter depends on the product of the first power of the aperture co-ordinate and the linear extent of the object. A recent example of a system with a magnification of 25 and a focal length of 12.5 cm showed primary transverse spherical aberration of 180 microns and an obliquity aberration of 4 microns for a 20 micron object. The latter result, namely small obliquity aberration relative to the spherical, is a fortuitous happening for the imaging of laser-fusion-pellets. If the focal length had been smaller the obliquity aberration could readily be greater than the spherical aberration.

Since past experience has shown that no conic section is a solution to the general aberration problem for finite distances and magnifications greater than one, it is natural to think in terms of perturbing the shape of the concave cylindrical-surface. An earlier analysis by McGee and Hesser (6) suggested using a concave cylindrical surface described by the polynomial

$$y = \frac{x^2}{2R_o} + \epsilon_o x^3 \qquad (1)$$

where ϵ_o is negative for $M > 1$, positive for $M < 1$ and zero for $M = 1$. The radius of curvature at $x = 0$ is R_o. The first term, which approximates a cylinder of large radius, yields a point spread function which is very un-symmetrical, tailing off monatonically and rapidly on the low angle side while oscillating with decreasing amplitude on the high angle side for hundreds of microns. However when the cubic term is added a symmetrical behavior similar to the far-field diffraction field of a single slit results. The end result is increased system resolution by at least an order of magnitude.

Instead of a diffraction analysis, similar to the one which showed that the addition of the cubic term of Eq. (1) was instrumental in removing a large amount of the spherical aberration, a geometrical analysis to determine the figure (shape) of the surface to powers higher than the third was undertaken. The new analysis has verified the dependence of the cubic coefficient on the system parameters and in addition has yielded the coefficients of several higher powers, in terms of the system parameters such as the radius of curvature R_0 at the origin, the magnification M, the object distance p and the grazing angle of incidence for the chief ray.

II. A. Reduction of Spherical Aberration by a Higher Order Polynomial Surface Figure

In Fig. 1, the chief ray p is shown originating at the point $x_0 y_0$ in the meridian plane of the concave reflector whose radius of curvature at the point C is R_0. Another ray p_1 is whown incident at point B to the left of the origin. The chief ray q forms its image at x,y in image space. The ray p_1 after reflection at B is labeled q_1 and passes through the point x,y. What is sought is a higher order polynomial giving the optimum shape $y_1 = f(x_1)$ which will cause all rays over a large aperture to pass through the point x,y. This is analogous to ray-tracing but done in a completely analytic manner. Instead of assuming a test surface-shape and then finding where several hundred or thousand rays go after reflection, the present analysis is aimed at finding the equation of the surface which will reflect many rays through a given point x,y whose position is determined beforehand by first order Gaussian optics.

The analysis starts with the vertical position of point B designated y_1. It is noted that $y_1 = s \sin \alpha_1$. The next step is to use the law of sines on the triangel BCD with the result that

$$\frac{s}{\sin \alpha_2} = \frac{q}{\sin(i_1 - \gamma_2)} \tag{2}$$

The labeling of the various angles involved requires an additional figure for clarity. By use of Fig. 2 it is seen that

$$\gamma_2 = 2\theta_1 - \phi + i_o \quad \text{and} \tag{3}$$

$$(i_1 - \alpha_2) = \phi - 2\theta_1 + \alpha_1 \tag{4}$$

so that Eq. (2) becomes upon solving for s

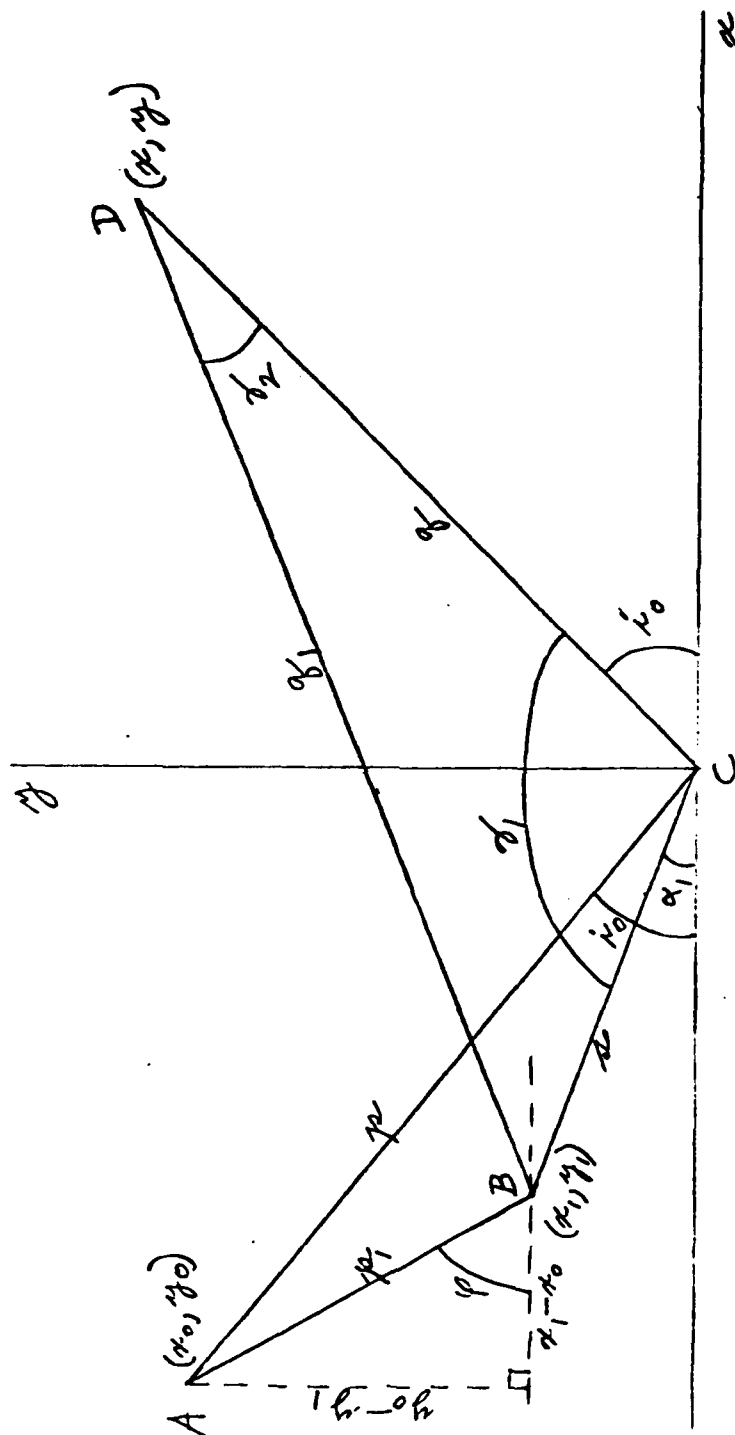$$s = q \; \frac{\sin (2\theta_1 - \phi + i_o)}{\sin (\phi - 2\theta_1 + \alpha_1)}$$

Fig. 1. Rays from a Point Object Reflecting from the Center and Left Side of a Mirror of Optimum Cross-Section

thus
$$y = q \; \frac{\sin(2\theta_1 - \phi + i_o)}{\sin(\phi - 2\theta_1 + \alpha_1)} \; \sin \alpha_1 \qquad (5)$$

With the aid of trignometric identities for the sine and cosine of the difference of two angles y_1 can be expressed as

$$y_1 = q \sin \alpha_1 \; \frac{\begin{array}{c}(\sin2\theta_1 \cos\phi \cos i_o + \sin2\theta_1 \sin\phi \sin i_o - \cos2\theta_1 \sin\phi \cos i_o \\ \ldots + \cos2\theta_1 \cos\phi \sin i_o)\end{array}}{\begin{array}{c}(\sin\phi \cos2\theta_1 \cos\alpha_1 + \sin\phi \sin2\theta_1 \sin\alpha_1 - \cos\phi \sin2\theta_1 \cos\alpha_1 + \ldots \\ \ldots + \cos\phi \cos2\theta_1 \sin\alpha_1)\end{array}} \qquad (6)$$

From Fig. 2 it can be seen that

$$\sin \alpha_1 = \frac{y_1}{\sqrt{x_1^2 + y_1^2}} \qquad\qquad \cos \alpha_1 = \frac{- x_1}{\sqrt{x_1^2 + y_1^2}}$$

Since BE is tangent to the reflector at B and makes an angle θ_1 with the x axis it follows that

$$\tan \theta_1 = - \frac{dy_1}{dx_1}$$

with the consequence that

$$\sin \theta_1 = \frac{dy_1}{\sqrt{(dx_1)^2 + (dy_1)^2}} \qquad \text{and} \qquad \cos \theta_1 = - \frac{dx_1}{\sqrt{(dx_1)^2 + (dy_1)^2}}$$

Since $\sin 2\theta_1 = 2 \sin \theta_1 \cos \theta_1$ and

$$\cos 2\theta_1 = 1 - 2 \sin^2\theta_1$$

it follows that

$$\sin 2\theta_1 = - \frac{2 \, dx_1 \, dy_1}{(dx_1)^2 + (dy_1)^2} = - \frac{2 \, \dfrac{dy_1}{dx_1}}{1 + \left(\dfrac{dy_1}{dx_1}\right)^2} \qquad (7)$$
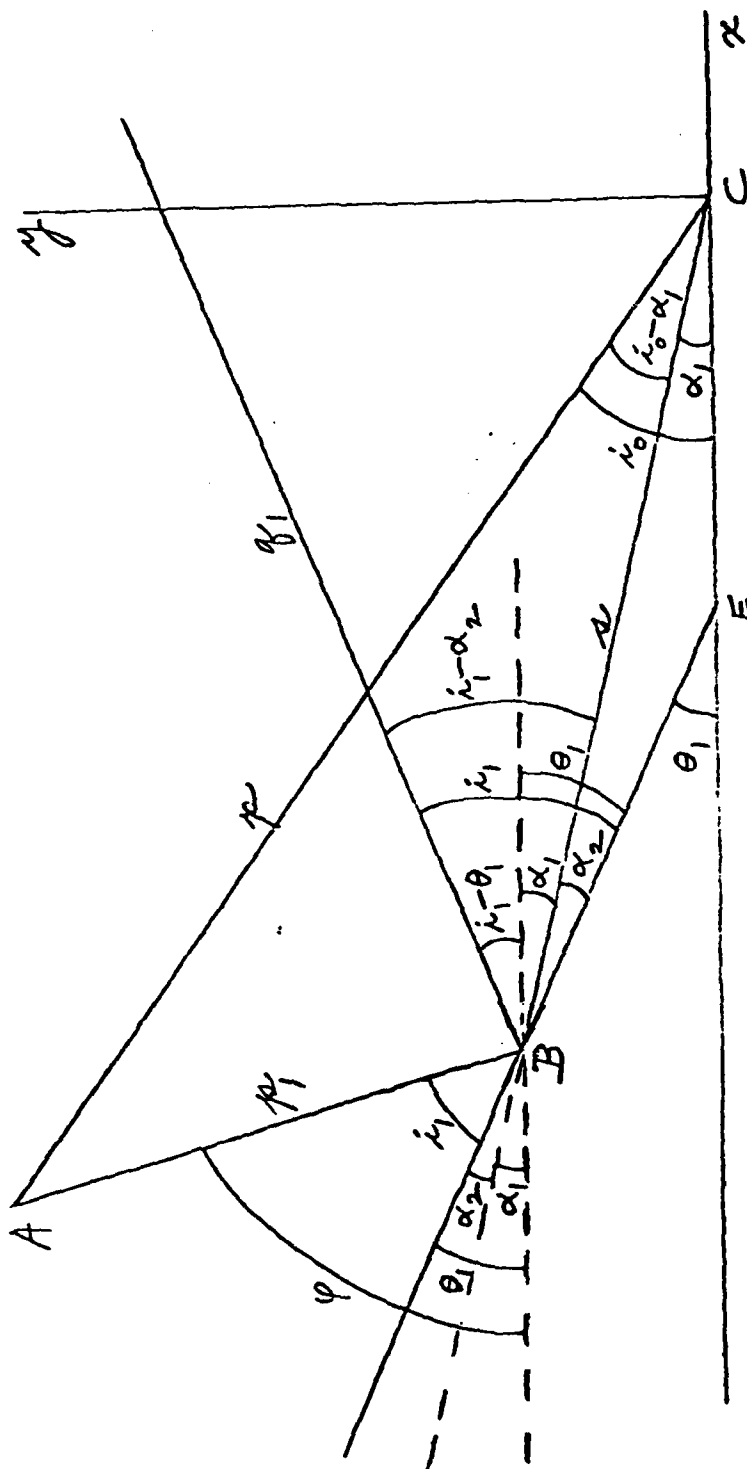
Fig. 2. Detail of a Portion of Fig. 1.

$$\cos 2\theta_1 = 1 - \frac{2(dy_1)^2}{(dx_1)^2 + (dy_1)^2} = \frac{1 - \left(\frac{dy_1}{dx_1}\right)^2}{1 + \left(\frac{dy_1}{dx_1}\right)^2} \qquad (8)$$

From Fig. 1 is is clear that

$$\sin \phi = \frac{y_o - y_1}{\sqrt{(x_1 - x_o)^2 + (y_o - y_1)^2}} \qquad (9)$$

$$\cos \phi = \frac{x_1 - x_o}{\sqrt{(x_1 - x_o)^2 + (y_o - y_1)^2}} \qquad (10)$$

Upon making the above substitutions for $\sin 2\theta_1$, $\cos 2\theta_1$, $\sin \phi$ and $\cos \phi$ into the y_1 expression the result is a rather involved differential equation of the first order and second degree. After several detailed algebraic steps the differential equation is finally put in a form suitable for solution by a standard method. Since only a few additional terms beyond the cubic term was desired it was decided to assume a solution in the form of a polynomial with eight terms. Therefore let

$$y_1 = \sum_{i=0}^{i=8} a_i x_1^i \qquad (11)$$

and
$$\frac{dy_1}{dx_1} = \sum_{i=0}^{i=8} i \, a_i \, x_1^{i-1} \qquad (12)$$

However from Fig. 1; $y_1 = 0$ and $\left(\frac{dy_1}{dx_1}\right)_o = 0$

so that $a_o = 0$ and $a_1 = 0$.

After substituting and equating the coefficients of like powers of x_1 in the resulting differential equation it was particularly gratifying to find that

- 7 -

Table 1

x_1 (cm)	y_1 (cm)	dy_1/dx_1	R_1 (cm)
-2.54	.00714	-.00593	365.3
-2.29	.00572	-.00525	378.2
-2.03	.00447	-.00459	391.3
-1.78	.00339	-.00395	404.4
-1.52	.00246	-.00333	417.7
-1.27	.00169	-.00273	431.1
-1.02	.00107	-.00215	444.7
-.762	.00060	-.00156	458.3
-.508	.00026	-.0010	472.1
-.254	.00006	-.0005	486.0
0	0	0	500.0
.254	.00006	.0005	514.0
.508	.00025	.00099	528.3
.762	.00056	.0015	542.6
1.02	.00099	.0019	557.0
1.27	.00154	.00237	571.5
1.52	.00220	.00281	586.1
1.78	.00297	.00324	600.8
2.03	.00384	.00365	615.6
2.29	.00482	.00407	630.5
2.54	.00591	.00446	645.5

$$a_3 = \frac{(1 - M) \cos i_c}{4 R_o M p} \tag{13}$$

which is in exact agreement with the coefficient ε_o of the cubic equation which was a direct result of a previous diffraction analysis (6). Additional coefficients were found to be

$$a_4 = \frac{5(1 - M)^2 \cos^2 i_c}{32 R_o M^2 p^2} + \frac{1}{8 R_o M p^2} \tag{14}$$

$$a_5 = \frac{7(1 - M)^3 \cos^3 i_c}{64 R_o M^3 p^3} + \frac{3(1 - M) \cos i_c}{16 R_o M^2 p^3} \tag{15}$$

Similar, but more involved expressions for a_6, a_7 and a_8 were found but have been omitted for the sake of brevity.

The polynomial

$$y = \sum_{i=2}^{i=8} a_i x^i \tag{16}$$

was evaluated for the range $0 < x < 5.08$ cm with $R_0 = 500$ cm, $p - 13$ cm, $i_o = .050$ radians and $M = 25$. The results are tabulated in Table 1. Over a range of 5.08 cm it is noted that the radius of curvature varies rapidly and widely from a low of 365 cm to a high of 646 cm.

II. B. Fabrication and Testing of Desired Surface

1. Since the radius of curvature varies on the average by 1.4 meters per cm of length, the making of such a small concave-surface presents problems. Already many grinding and polishing companies refused to bid on the job. While waiting for a suitable outside vendor we have gone ahead with the design of suitable grinding and polishing apparatus. One important consideration is that the tool area must be small in comparison with the work since the radius of curvature is to change rapidly in one direction (x). On the other hand there should be no tendency for grinding in the orthogonal direction (z). How this is presently being accomplished may be seen in the accompanying Fig. 3. The grinding head mounted on the ram of a machine-shop shaper contains a rotating glass cylinder; the tool is driven by a separate motor. Contact between the tool and the work is over a narrow straight line. Meanwhile, via the ram's head, the tool can be moved precisely over the work by hand operation of a crank on the shaper. A dial indicator with a range of three inches and reading directly to 0.0001 inch is connected to the ram's head for precisely locating the tool on the work.
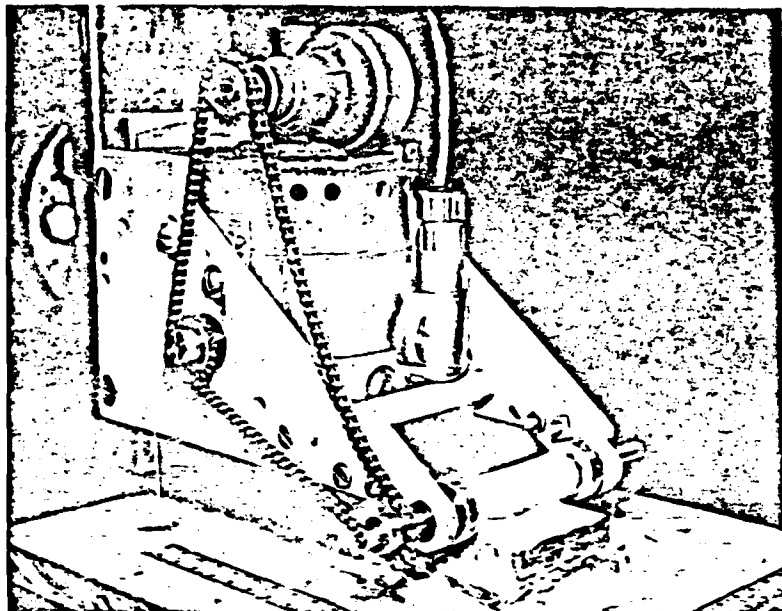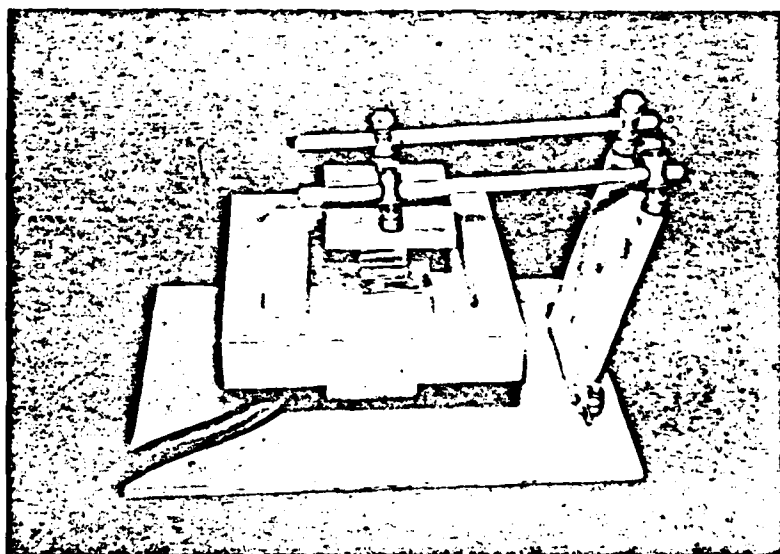
Fig. 3

Fig. 4

Another dial indicator, not shown, precisely determines the depth of the cut.

To know when the dimensions of Table 1 are being approached a dial gauge sensitive to 0.0001 inch is moved over the ground surface. The gauge mounted on the grinding table can be readily positioned for a sweep over any part of the concave surface being developed. The work, which is cemented to a steel plate which in turn is located on the grinding table by precision pins, can be removed for a more precise measurement on a Dia-Met machine which has a least count of 1×10^{-6} inches. With the exhaustion of mechanical and electromechanical measurements one turns to optical techniques.

2. In Fig. 4 may be seen the hand lapping machine recently built in our shop for the final finishing of the optical surfaces. Because of the universal joints, it is possible to produce a rotorary motion of the tool over the work. However, since zero optical power must be maintained in one direction most of the lapping will be done with only a minimum of sidewise motion unless called for due to small corrections in the desired figure.

3. A Tyman-Green type of interferometer is being readied for the purpose of optically checking the finished surface. The interferogram will reveal whether any curvature has been introduced in the zero power direction besides yielding values of the curvature versus distance x which with the aid of a computer can be used to check for the correct magnitudes of the coefficients in the polynomial describing the figure of the surface.

III. X-Ray Source Developments

For x-ray optical experiments at long x-ray wavelengths of 10 Å or greater the source of x-rays has historically presented various problems. Commercial sealed-off tubes such as used in x-ray crystallography are not available for good technical and economical reasons. Demountable pumped tubes are the answer and many laboratories make their own. But these are not without problems also. Many x-ray tubes operate with a tungsten filament in the region of 2500°K. The high operating-temperature results in evaporation of the filament material with two serious consequences. The first is a finite but relatively short lifetime. The second is contamination of the target and windows of the x-ray tube with tungsten. In addition, if the tube is of the demountable type, connected to an oil diffusion-pump and a mechanical fore-pump, then carbonaceous deposits can be a problem. In the typical tube, the filament is mounted within a centimeter or two of the target. The radiant heating of the target by the adjacent filament structure is a serious drawback especially with low melting-point targets. Many if not all of the above objectionable features are circumvented by a plasma controlled x-ray tube using a low pressure atmosphere of helium and essentially a cold cathode structure. While this may seem like a turning back of the clock to the era of gas tubes used so successfully by Seeman, Siegbahn, and Wyckoff to name a few, nevertheless the described tube has several features which distinguish it from earlier gas-type tubes. Its mode of operation is best described using the terminology of modern plasma physics. The "pinch" effect for example plays a large

role in controlling the beam diameter over a considerable distance. Generation of the plasma starts with positive ion bombardment of a cage-like cathode made of nickel mesh. While various cage shapes have been explored, a simple cylindrical basket with a hole in the bottom, on axis and facing the x-ray target, is adequate. With a sufficiently high voltage between the cathode and the target, the resulting positive-ion bombardment of the cathode structure produces secondary electrons within it. Due to penetration of the electric field in the vicinity of the hole or aperture in the cathode cage, electrons are extracted and accelerated toward the target, producing more ions on the way. A well defined luminous beam, approximating the diameter of the cathode aperture, develops between the cathode and the target. The remarkable uniformity of the beam's cross-section over a distance of ten or more inches may be explained by the pinch effect of plasma physics. As with many plasma phenomena, the start up and stability of the resulting plasma may be troublesome. Recently several modifications to insure its stability have been successful so that now the tube can be operated almost as routinely as a sealed-off hard x-ray tube. For the purposes of our long-wavelength x-ray optics experiments, the tube has been operated with an aluminum target at 15 kev and a current of 10 ma for long periods of time. A wide range of wavelengths and power inputs are possible.

IV. Recent Publications or Presentations

A. A tutorial type of paper titled "Properties of an X-Ray Catoptrical System" was presented at the Conference on Optics '79, which was held at Los Alamos, N.M., May 23-25, 1979. The paper will be published by S.P.I.E. in Volume 190 which bears the title Los Alamos Conference on Optics '79.

B. A paper titled "A Plasma Controlled X-Ray Tube" was presented at the 1979 Denver X-Ray Conference held July 30 through August 3, 1979 at the University of Denver. The paper has been accepted for publication in Volume 22, ADVANCES IN X-RAY ANALYSIS, by Plenum Publishing, N.Y.

Copies of the above are included in the last section of this report.

PROPERTIES OF AN X-RAY CATOPTRICAL SYSTEM*

James F. McGee
Saint Louis University
St. Louis, Missouri 63103

Abstract

The need for an x-ray imaging system with better than micron resolution is increasingly evident to workers in laser fusion and general plasma diagnostics. As early as 1974, John L. Emmett of the Lawrence Livermore Laboratories in an article titled, "Shopping List for Fusion" cited the need for hardware to make measurements with micron resolution in the soft x-ray region. In the same year, KMS reported that their x-ray image of an imploding pellet, formed with a pinhole, had a resolution of only 14 microns. Laser-fusion diagnostic requirements are such that it requires viewing a small object at neither very small or very large distances. What is needed is an x-ray microscope with a large working-distance objective. For this and other reasons we favor the basic Kirkpatrick-Baez arrangement. We shall explore some of the problems and solutions associated with the formation of x-ray images at small angles of grazing incidence mainly in the crossed-mirror configuration.

Introduction

In this country developments in x-ray reflection optics predates the needs of laser fusion, exploding wires and plasma research in general. Aside from crystallographic applications, x-ray focusing optics was mainly thought of in terms of x-ray microscopy as a possible alternative to the electron and light microscopes in the biological field. Sputnik and subsequent space-research requirements changed the emphasis somewhat to x-ray telescopes instead of x-ray microscopes.

The two most common types of x-ray focusing systems are the Kirkpatrick-Baez (1948) crossed-mirror system and the Wolter (1952) axial symmetric system of paraboloids and hyperboloids. It was the latter system that was adopted for space research. Both systems have formidable problems associated with them.

Matter is not very refractive to x-rays and the hope of developing an x-ray microscope along the lines of light optics was defeated for many years by statements due to Röntgen himself. His early experiments convinced him that the new rays could not be concentrated by lenses. For example an ordinary spectacle lens would have a focal length of a hundred kilometers assuming of course that the radiation was not completely absorbed by the lens itself or the intervening atmosphere. Although matter does not refract x-ray appreciably it will however reflect them. The success of modern x-ray reflection optics depends upon the basic physical fact that the index of refraction of matter in the x-ray region is slightly less than one. As a consequence x-rays are totally reflected in going from a less dense medium to a more dense one, provided that the angle of incidence θ is approximately no less than 87°. In x-ray reflection optics it is customary to use the angle of grazing incidence i which is the complement of the conventional angle of incidence. Hence if x-rays in air graze any surface by an angle less than 3° they may be totally reflected into the air region depending among other things on the wavelength of the incident x-rays.

Crossed-Mirror X-Ray Optics

X-ray reflection optics as we know it today had its beginning with the realization by Jentzsch[1] that a concave mirror surface would focus x-rays at grazing incidence. He derived the following formulae for the tangential (meridian) and sagittal rays.

$$\frac{1}{p_t} + \frac{1}{q_t} = \frac{2}{R \sin i} = \frac{1}{f_t} \tag{1}$$

$$\frac{1}{p_s} + \frac{1}{q_s} = \frac{2 \sin i}{R} = \frac{1}{f_s} \tag{2}$$

where p and q are object and image distances respectively, i is the angle of grazing incidence and R is the radius of curvature of the concave reflecting surface. He was disappointed to find that a high degree of astigmatism was present so that he was led to the conclusion that a single reflecting surface was useless to image an anticathode or a slit diaphragm as he had hoped. He did nevertheless show that for the case of grazing incidence, the demands on mirror quality for x-rays are not very different than in the visible region at normal incidence. Since the roughness h should not exceed $\lambda/8 \sin i$, it is apparent that the small angle i offsets the small wavelength of x-rays. For example if $\lambda = 8.34$ Å and i = .050 radians, the surface roughness should not exceed 20 Å, an attainable value.
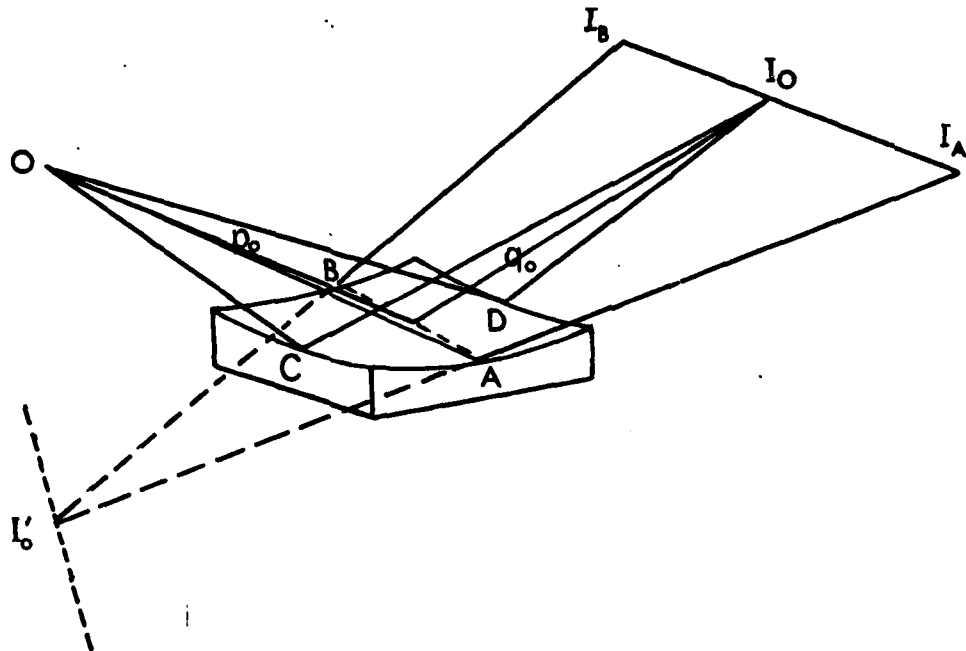
Fig. 1. Grazing-incidence optics of a single concave reflector of large radius of curvature. The image of a point object is a highly astigmatic line perpendicular to the plane of incidence. Sagittal rays give rise to a virtual line image. The ratio of focal lengths $f_s/f_t = 1/i^2$ is very large.

In Fig. 1 the fan of rays from O determined by the equatorial arc AB is called the sagittal fan while the rays determined by O and the meridian arc CD is the tangential or meridian fan. All tangential rays such as OA and OB are governed by Eq. (1). The ray OA determines the image point I_A while the ray OB determines the image point I_B. The image of O formed by the chief ray p_o through the center of the reflector is I_o. Thus the real image of O is the astigmatic line $I_A I_o I_B$. If the lines AI_a and BI_B are extrapolated backwards they will intersect in a virtual focus point at I_o' the position of which is given by Eq. (2). If other arcs parallel to AB are used to determine the fan of sagittal rays it will be found that the virtual image points lie along a line perpendicular to the real image line.

This objectionable astigmatism, the despair of Jentzsch, was subsequently removed to first order by Kirkpatrick and Baez[2] who placed two similar concave reflectors one behind the other in the crossed configuration shown in Fig. 2.
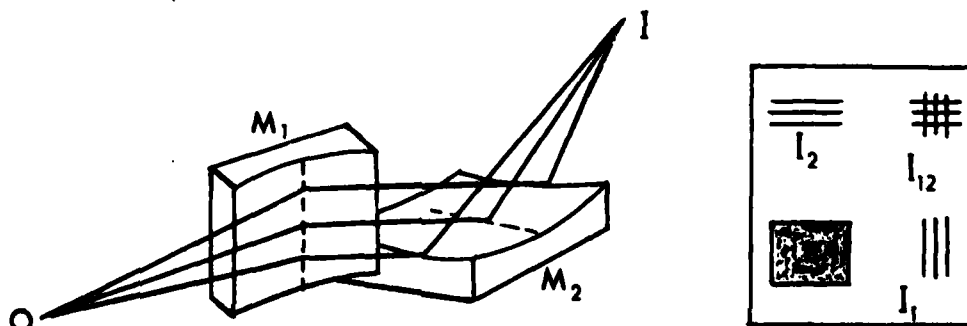

Fig. 2. A practical method of correcting the astigmatism of a single reflector is by crossing two identical concave cylindrical reflectors so that their meridian planes are at right angles to each other.

It has been shown by Montel[3] for the case of grazing incidence and mirrors crossed as in Fig. 2 that on average each mirror focuses only rays lying in its plane of incidence and is ineffective for focusing rays lying in a perpendicular plane. The image formed by the tangential rays of mirror M_2 depends only on M_2 and the sagittal rays helping to form the stigmatic image depend only on mirror M_1. If the point object at 0 is replaced by a backlighted grid then typically four blackenings occur on the recording film. Three are images while the fourth is the result of the direct beam missing both reflectors. Rays which are reflected only by M_1 produce a focused image of the vertical grid bars as I_1; rays which are reflected and focused by M_2 produce a focused image of the horizontal bars at I_2. Rays which are reflected by both M_1 and M_2 form the complete image of the grid at I_{12}.

Because each mirror operates independently of the other, under a sufficiently small-angle approximation, it is possible to make a two-dimensional analysis of the aberrations associated with a single reflecting surface.

Spherical Aberration

If one looks critically at the intensity distribution in the meridian plane of the line image shown in Fig. 1, it will be seen to trail over a large distance in the direction of increasing reflection angle. The apparent broadening of such a line image was early noted by Ehrenberg[4] and later shown by McGee[5] to be due to diffraction in the presence of a large amount of spherical aberration. Ehrenberg's early experiments with the image of a slit showed a relatively sharp image for an exposure time of 2 seconds. Exposures of 20, 200, 2000, and 20,000 seconds resulted in increasingly broader images. Broadening with increased exposure time is to be expected if the diffraction image has the general features of the one shown in Fig. 3.

In Fig. 3, the dotted line shows the position of the geometrical focus according to Eq. (1). The broadening in some cases can amount to hundreds of microns. It has been shown by McGee[6] that by figuring the surface of the reflector so that it is represented by Eq. (3) a large amount of the spherical aberration can be removed.

$$y = \frac{x^2}{2R_o} + \epsilon_o x^3 \qquad (3)$$

When a reflector described by Eq. (3) is illuminated by a point source the diffraction image has a complete change of character. It is symmetrical and its width at half-maximum is very much smaller as seen in Fig. 4.
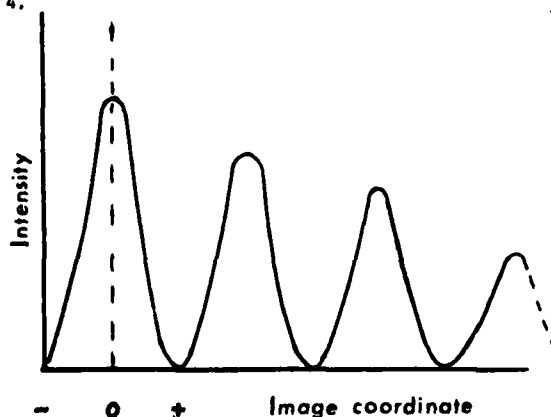

Fig. 3. Intensity distribution in the diffraction image of a point source produced by a concave cylindrical section of large radius of curvature R and large apertures.
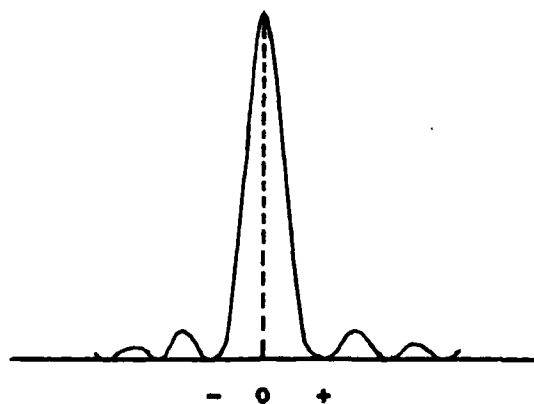
Fig. 4. Intensity distribution upon addition of the cubic perturbation term to the cylindrical surface of large radius of curvature.

The diffraction pattern is so superior that the resolution of the reflector is increased by at least an order of magnitude over that obtainable by a simple spherical reflector or cylinder of circular section.

A recent geometrical analysis by McGee and Burrows[9] succeeded in extending the cubic polynomial representing the desirable figure. The latter analysis confirmed the coefficient ϵ_o of the third order or cubic term of Eq. (3).

$$\epsilon_o = \frac{(1-M)}{4R_o Mp} \cos i \qquad (4)$$

as previously given by a diffraction analyses by McGee, Hesser, and Milton.[6] The coefficients expressed in terms of common system parameter M, magnification; R_o, radius of curvature; p, object distance and i, grazing angle of the chief ray are available for all powers of the polynomial up to and including the eighth.

It is interesting to note that for magnification M greater than unity the value of ϵ_o is negative while for M less than unity it is positive. In keeping with this change of sign it has been noted that the tailing off to the high reflection angle of the line image of Fig. 1 occurs only when the magnification is greater than unity. If the magnification is made less than unity then the image trails off to the low angle side. Thus the change in sign of the coefficient of the cubic term would compensate for the new situation. McGee and Milton[7,8] made a ray-tracing study which shows the reversal when the magnification changes from above to below unity. A diffraction analysis to determine what gain, if any, in resolution is to be had by adding one or more high-power terms to the polynomial has been undertaken in our laboratory.

The Obliquity Aberration

Since the crossed mirror system has no axis of symmetry, the chief ray has served as a reference axis in the preceding discussions. If at point 0 of Fig. 2 a small line object is oriented perpendicularly to the chief ray in object space, what becomes of its image? The answer as shown in Fig. 5 is that it will be inclined severely toward the chief ray making an angle $\gamma \equiv i/M$ with it.
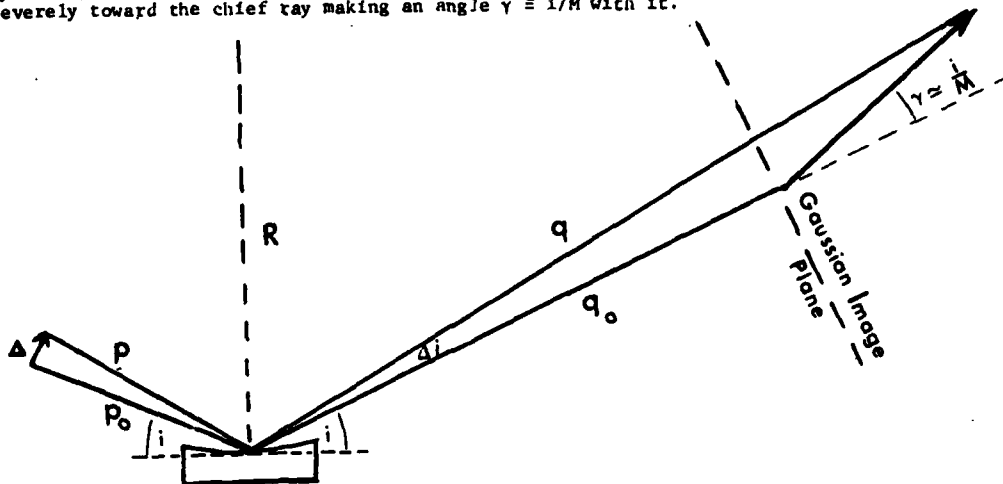

Fig. 5. A small line object of extent Δ is not perfectly imaged in the Gaussian plane as a line of length $M\Delta$ where M is the magnification q/p. Instead the image is severely inclined toward the chief ray as shown making an angle $\gamma \simeq i/M$ with it.

A simple calculation will help to reveal the extent of the problem. With an assumed $p_o = 8$ cm; i = .050 radians and R = 300 cm, the image distance $q_o = 119.206$ cm and the magnification M = $q_o/p_o = 14.901$. A line object of extent $\Delta = .0080$ cm would produce a $\Delta i = .001$ radian. With p = p_o and i = .051 radians the image distance q = 173.141 cm. Thus the head of the arrow is imaged some 53.935 cm behind the Gaussian image plane. The magnification M = q/p = 21.642 for the latter case. The above numbers yield $\gamma = .0032$ radians = i/M.

The Comatic Aberration

The above calculation reveals another serious defect arising from the lack of constant magnification. If a narrow fan of rays is traced from the arrow head in object space to its corresponding image-point it will intersect the Gaussian image plane over a finite distance δ, called the blur. The fan of rays from the bottom of the arrow, on the other hand, will by Gaussian optics have zero blur in the Gaussian image plane. For points between these extremes, the blur will vary from a maximum to a mimimum of zero. In a two-dimensional image plane these would give rise to the familiar tear drop shape. The comatic aberration depends on the distance Δ of the point from the chief ray and the square of the aperture angle u (not shown in Fig. 5). If u and u' are the aperture angles in object and image space respectively then the condition that the system be free of coma is given by the Abbe's sine condition, M = sin u/sin u', for all object points. Spherical aberration is then also zero. The system is said to be aplanatic. Coma has been defined as spherical aberration of a point off the axis. The larger the field of view one requires the more serious the coma consideration becomes.

Conclusion

The anticipated limit of resolution of an x-ray microscope with platinum coated reflectors is about 70 Å.

This places the x-ray microscope midway between the electron microscope and the visible light microscope with respect to its resolution limit. Before this limit can be obtained however there are many problems remaining. The control of coma is extremely important. A most likely solution lies in the use of a compound system (more than two reflectors), aperture stops and aspheric surfaces. When more detailed knowledge becomes available as to how each system parameter affects the coefficient of each aberration defect, the possibility of balancing off one positive defect against a negative one should become apparent.

References

1. Jentzsch, F., Phys. Z., Vol. 30, p. 268. 1929.
2. Kirkpatrick, P. and Baez, A. V., J. Opt. Soc. Am., Vol. 38, p. 766. 1948.
3. Montel, M., Optica Acta, Vol. 1, p. 117. 1954.
4. Ehrenberg, W., J. Opt. Soc. Am., Vol. 39, p. 741. 1949.; J. Opt. Soc. Am., Vol. 39, p. 746. 1949.
5. McGee, J. F. and Olli, V. I., Advances in X-Ray Analysis, Vol. 10, p. 108, Plenum Press 1967.
6. McGee, J.F., Hesser, D. R., and Milton, J. W., Vth International Congress on X-Ray Optics and Microanalysis, edited by Möllenstedt, G. and Gaukler, K. H., Springer-Verlag, Berlin 1969.
7. McGee, J. F. and Milton, J. W., unpublished.
8. McGee, J. F. and Milton, J. W., X-Ray Microscopy and Microanalysis, edited by Engström, A., Cosslett, V. E., and Pattee, H. H., Elsevier, Amsterdam 1960.
9. McGee, J. F. and Burrows, J. W. W., X-Ray Imaging, Vol. 106, p. 107, S.P.I.E. Press 1977.

A PLASMA CONTROLLED X-RAY TUBE*

James F. McGee and Timo Saha**

Saint Louis University

St. Louis, Missouri 63103

ABSTRACT

Many x-ray tubes, used by crystallographers and others, operate
with the aid of a tungsten filament in the region of 2500°K. The
high operating temperature results in evaporation of the filament
material with two serious consequences. The first is a finite but
relatively short lifetime. The second is contamination of the tar-
get and windows with tungsten. In addition, if the tube is of the
demountable type, connected to an oil-diffusion pump and a mechani-
cal fore-pump, carbonaceous deposits can be a problem. In a typi-
cal tube, the filament is mounted within a centimeter or two of the
target. The resulting radiant heating of the target presents addi-
tional cooling problems especially with low melting-point targets.
Many if not all of the above objectional features are circumvented
by a plasma controlled x-ray tube using a low pressure atmosphere
of helium and a cage-like cathode fabricated from nickel wire-mesh.
An experimental model has been operated for several hours at 15 kv
and 10 ma on an aluminum target. Scaling up of the apparatus will
permit power dissipations in the kilowatt range limited mainly by
the available power source or vaporization of the target material.

INTRODUCTION

The plasma controlled x-ray tube is basically a gas-type
tube[1,2] unlike the more conventional Coolidge or high-vacuum sealed-
off tubes used in x-ray crystallography and elsewheres. Histori-

cally, gas tubes were used successfully by Seeman, Siegbahn, Wyckoff and other well known x-ray crystallographers and x-ray spectroscopists. While high vacuum x-ray tubes enjoy the advantage of independence of the applied voltage and current settings, they nevertheless have some well known drawbacks for general use. Their filament lifetime is finite and often very short. The tungsten evaporated from the filament will coat the target thereby changing the spectral output. Coating of the window of the x-ray tube results in reduced output due to absorption. The latter can have serious consequences in the case of quantitative experiments unless the output is separately monitored. For a target with fixed cooling capacity the radiant heating of the target by the filament limits the x-ray power which can be extracted from the target.

THE ANODE STRUCTURE

The plasma controlled x-ray tube like most x-ray tubes of uncomplicated design is basically a diode with an anode and a cathode which are contained in a glass and metal envelope. The latter may be highly evacuated as in the Coolidge type of tube or may contain gas at a pressure determined by the overall operating conditions. The anode of the experimental tube is made from copper with the usual provision for circulating a coolant, ethylene glycol, through several feet of Tygon tubing from a refrigerating system. This arrangement permits the target to be operated at high voltages without significant loss of current through the high electrical impedance of the cooling lines. The anode was cut so as to provide a flat surface oriented at 45° to the electron beam with provisions for a window placed so as to receive the x-rays emerging in the vicinity of 45° to the face of the anode. For the production of the aluminum Kα lines, a thin sheet of aluminum was soldered to the copper anode. Longer or shorter K lines are available by attaching with good thermal contact other materials of appropriate Z number.

THE CATHODE STRUCTURE

In general the cathodes were formed from 30 to 50 mesh nickel screen. Molybdenum screening if available would have been more suitable. Cathodes have been made in a variety of shapes mainly hollow cylinders, spheres and cones. These cathodes are to be distinguished from the hollow cathodes made of solid material which are used as high intensity radiation sources by spectroscopists (non-x-ray). Such cathodes operate at less than the kilovolt range and at high currents so are basically a low impedance device. The structure shown at B in Fig. 1 represents a cylindrical cathode. The end facing the target T has a hole approximately 1/4 inch in diameter symmetrically located on axis. The other end of the wire basket is connected to a metal rod which passes through a high voltage insulator in the metal end plate which is suitably attached
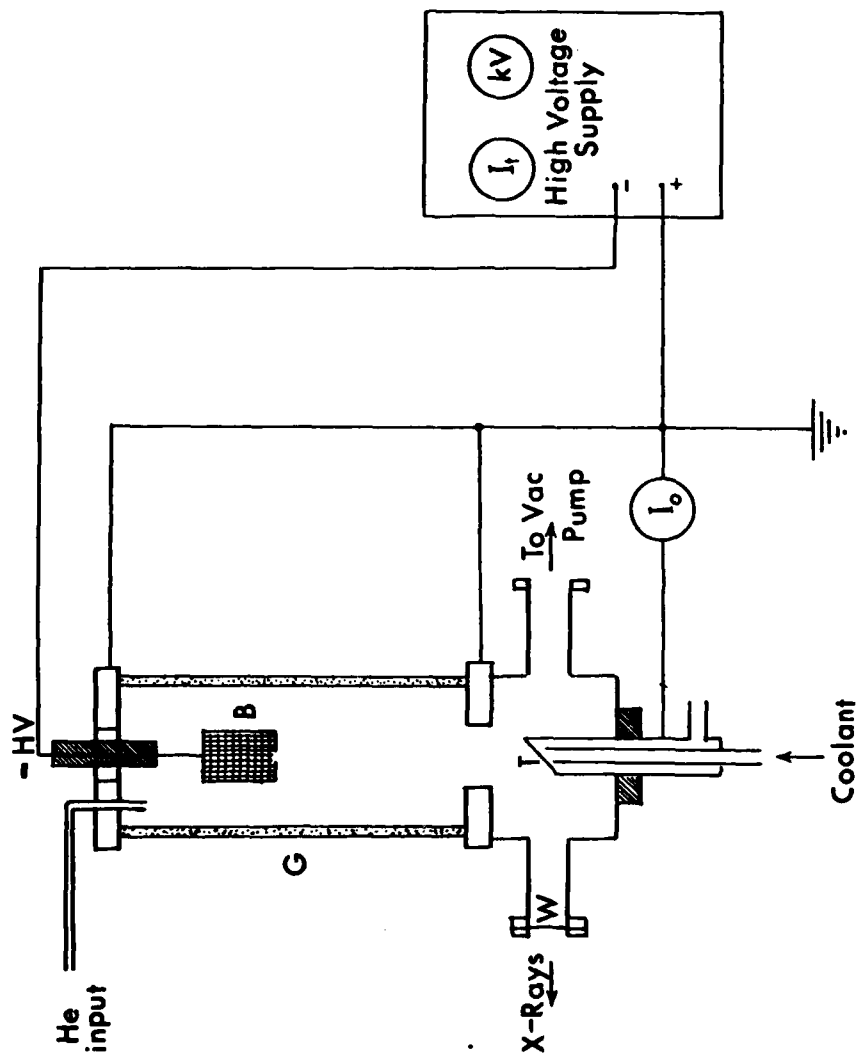
Fig. 1. The glass housing G of the x-ray tube is a 4 x 12 inch Pyrex tube (Corning). The smaller flanges are standard Ultek high-vacuum components. The target support-structure is a modified high-current water-cooled lead-through also by Ultek. Since the lead-through is insulated from the standard flange the actual current to the target I_o is readily measured. The hollow wire-mesh basket at B is in the form of a cylinder 2 inches long and 2 inches in diameter. It is made from #40 mesh nickel. The remaining components were fabricated in our shop.

to the glass envelope G. The latter is a Corning process glass-pipe measuring 12 inches in length and 4 inches in diameter. The dimensions of a basket currently in use are 2 inches in length and 2 inches in diameter with a 1/4 inch aperture in the bottom.

PRINCIPLE OF OPERATION

As indicated in Fig. 1, provision is made in the top of the tube for the entry of helium from a throttling valve. A vacuum pump continually removes the gas. By appropriate adjustment of the throttling valve, preferably by a simple servo system receiving its signal from the emission current, the pressure can be maintained at some nominal operating value, e.g., 30 microns. The application of a potential difference of a few thousand volts between the cathode B and anode T causes the few positive ions already present to be accelerated toward the cathode B. The bombardment of the cathode surfaces produces secondary electrons within the basket structure. Because of the hole in the bottom face of the basket the electric field penetrates the aperture to remove and help focus the electrons into a beam which is accelerated toward the target T of Fig. 1. Electrons outside the basket would be accelerated away from the cathode and subsequently may collide with neutral gas molecules to create more positive ions. Others may strike the glass walls and cause it to fluoresce and heat up. Experimentally one observes a greenish-blue column about 1/4 to 1/2 inch wide originating in the basket and terminating at the surface of the target. As evidenced by the fact that x-rays are emitted and that the greenish-blue beam can be deflected by a magnet it obviously contains electrons. The fact that the beam does not significantly diverge over a distance of eight or more inches suggests that some constraining force is at work.

ELEMENTS OF PLASMA PHYSICS

Imagine a cylindrical column of plasma in existence between plane and electrodes raised to a potential difference V. The established electric field E causes the current I to flow parallel to the axis of the cylinder. In virtue of Ampere's circuital law a tangential magnetic field of induction B encircles the current. If v is the particle velocity in the same direction as the current, the Lorentz force v x B will be in a radial direction helping to contain the charged particles within the column. This is the well known pinch effect of plasma physics. Should some small variation in cross section of the beam occur, then the beam will experience a stronger inward push since B varies inversely with radius. The result is that the perturbation is enhanced and instability sets in. Much has already appeared in the literature on the subject of plasma physics including the subject of stability. The reader may find the three volumes Reviews of Plasma Physics, edited by M. A. Leontovich and published by Consultant's Bureau, N. Y. 1965, an

interesting introduction to the subject.[3]

OPERATION MODES

     If the pressure of helium in the x-ray tube is maintained in
the vicinity of 100 to 1000 microns then the discharge is of the
ordinary glow type described in many text books on atomic physics.
Anode voltages of less than one thousand volts easily produce cur-
rents exceeding the capability of ordinary high-voltage power sup-
plies at lower pressures of the order of 50 microns or less at least
two different modes of operation are possible. In either mode the
path of the electron beam is made visible by the luminescence of the
excited helium atoms along its path. Typically the beam cross-
section is approximately the size of the aperture in the cathode.
However pressure and the applied potential difference are also a
factor in determining the beam diameter. The graphs of Fig. 2 give
typical operating voltages and target currents for operation in
each of two modes A, B at 12 and 21 microns of pressure respective-
ly.
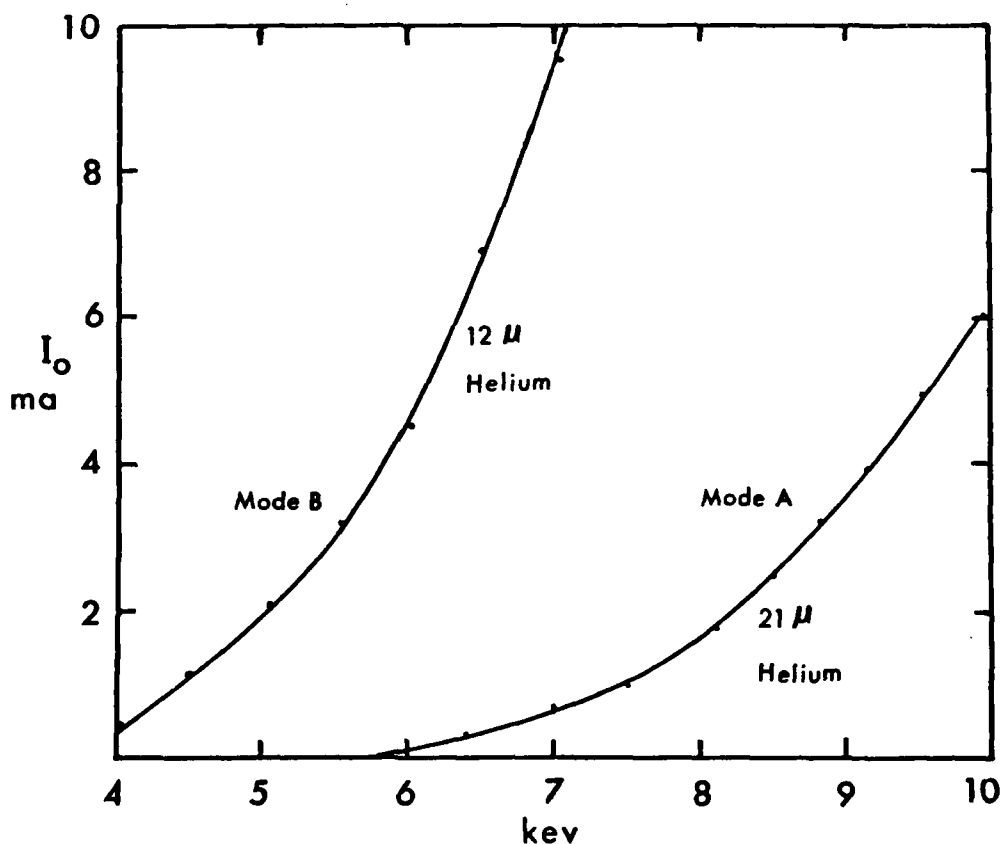
Fig. 2.   Characteristic curves of target current I_o versus target
potential at constant gas pressure. Two distinct modes are
evident.

Fig. 3. Energy spectrum recorded with tube operating at a poten-
tial difference of 8.61 kev and a target current of 5 ma.
The spectrum was recorded using a proportional counter
with P-10 gas and a North American Philips' multi-channel
analyser (IC 2000 Series). So as not to exceed the per-
missible counting rate of the proportional counter, a
pin-hole was used.

ENERGY SPECTRUM

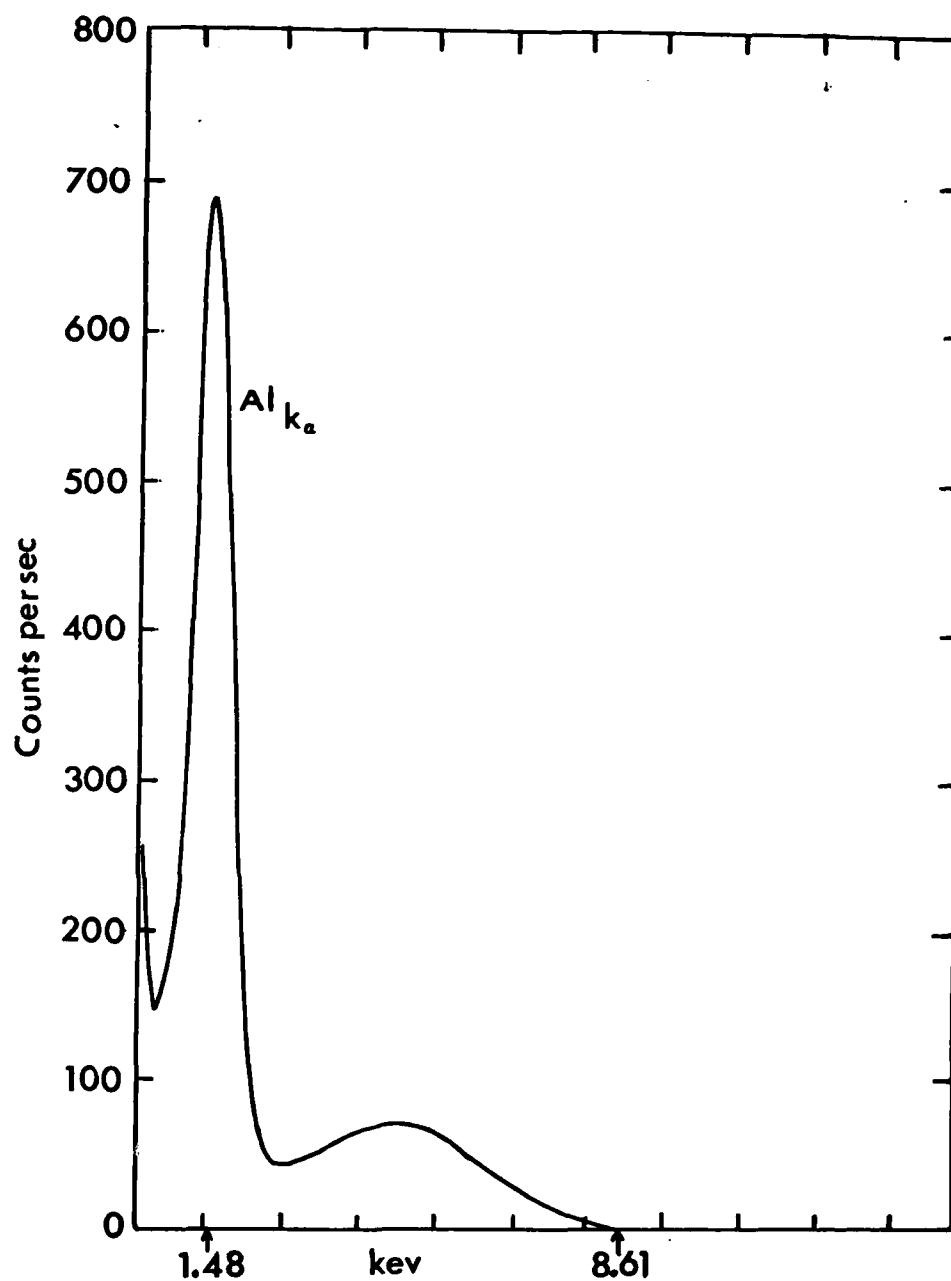The window of the x-ray tube was made from aluminum foil 0.00045 inch thick. It covers an aperture of 0.25 inch diameter. An energy spectrum derived from a proportional counter filled with P-10 gas is shown in Fig. 3. The actual spectrum was made with a North American Philips' multichannel analyser (IC 2000 Series). Within the limits of resolution of the recording apparatus the spectrum appears free of any contaminating radiations, showing only the unresolved Kα lines of aluminum and the Bremsstrahlung. As indicated the applied potential was 8.6 kev with a tube current of 8 ma. The resulting high intensity of x-rays was cut down by inserting a small pin-hole at the window of the x-ray tube so as not to exceed the counting rate of the proportional counter.

CONCLUSIONS

A gas discharge tube whose electron beam is controlled by plasma dynamics has been shown to be operable at power inputs comparable with many sealed off Coolidge type x-ray tubes with low atomic number targets such as vanadium and chrome. Unlike the tungsten filament type, the wire mesh cathode is almost indestructible under ordinary use. Contamination of the target is greatly reduced. Physical scaling of the cathode structure makes it possible to operate at much higher power inputs limited of course by the possible vaporization of a particular target if the power density to it becomes excessive.

REFERENCES

1. Solomon, J. S. and Baun, W. L., Rev. Sci. Instrum. 40, 1458-60 (1969).
2. Vanhatalo, J., Kaihola, L., and Suoninen, E., Journal of Physics E: Scientific Instruments 9, 1156-57 (1976).
3. Leontovich, M. A., editor, Revi_ws of Plasma Physics, Consultant's Bureau, N. Y. 1965.

Biographical Sketch:

Name	Title
McGee, James F.	Professor

Place of Birth	Nationality	Sex
Philadelphia, Pennsylvania	U.S.A. citizen	Male

Education

B.S.	1938	Physics	St. Joseph's College, Philadelphia, Pa.
M.S.	1940	Physics	University of Notre Dame, Indiana
Ph.D.	1956	Physics	Stanford University, California

Honors

Fulbright Professor of Physics, Finland, 1964-65
President, Sigma Xi (Saint Louis Chapter), 1968-69
Gold Medal for Mathematics, St. Joseph's College

Major Research Interest	Role in Proposed Project
X-ray Optics	Principal Investigator

Research Support

Previous: Research Corporation, National Science Foundation,
American Cancer Society, and National Institutes of Health

Current: Air Force Office of Scientific Research

Research and/or Professional Experience

1969-present	Professor of Physics, Saint Louis University
1959-1969	Associate Professor, Saint Louis University
1956-1959	Assistant Professor, Saint Louis University
1955-1956	Research Associate, Stanford University
1952-1955	Research Assistant, Stanford University
1949-1952	Research Engineer, Atomics International Division of North American-Rockwell
1946-1949	Research Engineer, Aerophysics Division of North American-Rockwell

Biographical Sketch:

Name   **Title**

  Ritva A.M. Keski-Kuha   Research Assistant

Place of Birth   **Nationality**   **Sex**

  Finland   Finnish   Female

Education

  B.S.   1976   Physics   University of Turku, Finland

  M.S.   1977   Physics   University of Turku, Finland

Major Research Interest   **Role in Proposed Project**

  X-Ray Optics   Research Assistant

Research and Professional Experience

  1978-79   Research Assistant   Saint Louis University   Research
  1977-78   Research Assistant   University of Turku   Research & Teaching

Publication

  "Total Reflection of X-Rays from the Transition Metals Fe, Cu, and Co
  Close to Their L-Absorption Edges," Proceedings of the Annual Conference
  of the Finnish Physical Society, 1978.

Biographical Sketch:

Name

Timo T. Saha

Title

Research Assistant

Place of Birth

Finland

Nationality

Finnish

Sex

Male

Education

B.S.	1974	Physics	University of Turku, Finland
M.S.	1975	Physics	University of Turku, Finland

Major Research Interest

X-Ray Optics

Role in Proposed Project

Research Assistant

Research and Professional Experience

1978-79	Research Assistant	Saint Louis University	Research & Teaching
1977-78	Research Assistant	University of Turku	Research & Teaching
1974-75	Research Assistant	University of Turku	Research & Teaching

Publications

"Electron Microscope Analysis of Epitaxially Grown Fe_2O_3 Crystals," Proceedings of the Annual Conference of the Finnish Physical Society, 1977.